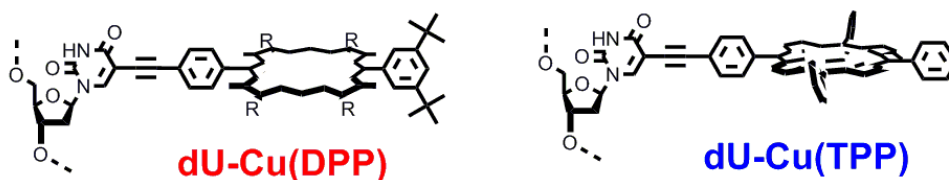


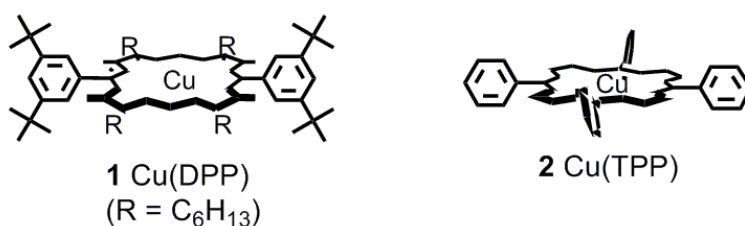
Electronic Supporting Information

1 EPR based distance measurement in Cu-porphyrin-DNA

ThaoNguyen Nguyen, Pär Håkansson, Ruth Edge, David Collison, Bernard A. Goodman, Jonathan R. Burns, Eugen Stulz



ODN1 5'-CAT CGT AGT ATA **TPT** ATA TCC GTA CTC-3'
ODN2 5'-CAT CGT AGT ATA **PAP** ATA TCC GTA CTC-3'
ODN3 5'-CAT CGT AGT ATA **PAT** ATA TCC GTA CTC-3'
ODN4 5'-CAT CGT AGT ATA **PAP** ATA TCC GTA CTC-3'
ODN5 5'-CAT CGT AGT **ATP** **PAT** ATA TCC GTA CTC-3'



2 General procedure for copper metallation of porphyrin-DNA

The porphyrin-DNA was synthesised as published in our previous report.¹ Cu(OAc)₂·H₂O (25 μL, 16 mM, 400 nmol, 200 eq.) was added to the porphyrin-DNA (100 μL, 10 μM, 2 or 4 nmol porphyrin equivalent) and immediately deoxygenated by purging with N₂ for 10 seconds, then stirred vigorously on a thermomixer at 85 °C for 5 min. The reaction mixture was then left to cool to room temperature for 5 min. EDTA pH 8.0 (100 μL, 400 mM, 40 μmol, 20000 eq.) was added to quench excess Cu(OAc)₂, followed by buffer (100 μL, 100 mM NaCl, 50 mM KH₂PO₄, pH 7.0). 6 batches of this reaction were performed simultaneously, combined, followed by addition of water (200 μL) and the reaction mixture was purified *via* Glen-Pak cartridge to give copper metallated DNA (averaged 93 %) as a dark purple solid. **ODN1**: UV-vis (H₂O, c= 5×10⁻⁶ M): λ_{max} (log ε) 261 (5.28), 410 (4.17) nm; Emission (H₂O, c= 5×10⁻⁶ M): λ_{ex} 410 nm, λ_{em} (rel int) 632 (1), 693 (0.96) nm. **ODN2**: UV-vis (H₂O, c= 5×10⁻⁶ M): λ_{max} (log ε) 265 (5.38), 409 (5.37) nm; Emission (H₂O, c= 5×10⁻⁶ M): λ_{ex} 409 nm, λ_{em} (rel int) 637 (1), 695 (0.75) nm. **ODN3**: UV-vis (H₂O, c= 5×10⁻⁶ M): λ_{max} (log ε) 260 (5.46), 422 (4.81) nm; Emission (H₂O, c= 5×10⁻⁶ M): λ_{ex} 422 nm, λ_{em} (rel int) 651 (1), 713 (0.32) nm. **ODN4**: UV-vis (H₂O, c= 5×10⁻⁶ M): λ_{max} (log ε) 264 (5.46), 423 (5.14) nm; Emission (H₂O, c= 5×10⁻⁶ M): λ_{ex} 423 nm, λ_{em} (rel int) 656 (1), 713 (0.35) nm. **ODN5**: UV-vis (H₂O, c= 5×10⁻⁶ M): λ_{max} (log ε) 260 (5.49), 423 (5.28) nm; Emission (H₂O, c= 5×10⁻⁶ M): λ_{ex} 423 nm, λ_{em} (rel int) 654 (1), 716 (0.28) nm.

3 EPR spectroscopy

All samples of copper porphyrin building blocks were investigated under three separate conditions: pure solid powder, fluid solution and frozen solution. Cu-porphyrin-DNA complexes were only measured as frozen solutions at 120 K, because of limited sample availability for pure solid measurements and the high molecular mass which produced rigid limit spectra from fluid solutions. For porphyrin building blocks DCM, and DCM:toluene 9:1 were used as solvents for fluid and frozen solution spectra, respectively, and Cu-porphyrin-DNA complexes were investigated in DNA grade water.

The EPR spectra were acquired using Bruker EMX-X band (approx. 9 GHz) and Bruker EMX Micro-X band (approx. 9 GHz). Low temperature spectra were acquired with variable temperature cryostats using liquid nitrogen as coolant for measurements in the temperature range 120 – 301 K. All samples were measured in quartz tubes with internal diameters of 3 mm (X-band). Spectra were acquired with 100 kHz modulation frequency in the field range 0 – 8000 (X-band) Gauss using the Bruker WIN-EPR program. Initial peak positions were estimated using WIN-EPR and these were then used to provide a basic interpretation of the spectra; all hyperfine coupling constants (A_{iso} , $A_{//}$, A_{\perp}) are quoted in Gauss.

4 Parameter estimation for copper porphyrin building blocks

The frozen solution EPR experiment (120 K) is analysed with the solid state line shape function (pepper) in EasySpin.² The pepper function allows for a computed powder average using second order perturbation theory for ¹⁴N ligands and matrix diagonalization for electronic energy levels. The spin Hamiltonian in pepper includes electron Zeeman, the ⁶³Cu(II) and ⁶⁵Cu(II) isotropic nuclear Zeeman (weighted at natural abundance ratio), Cu(II) Hyperfine and four ¹⁴N superhyperfine interactions. The routine pepper provides line broadening to mimic a frozen solution spectrum. Isotropic broadening of Gaussian form is used. Anisotropic parameters have a cylindrical symmetry as is expected for a square planar complex. In this work the inhomogeneous broadening of the so-called H-strain, g-strain are used. Minimization of

$$\chi^2 = \frac{1}{N} \sum_{i=1}^N \frac{(I'(B_i)_{EXP} - I'(B_i)_{SIM})^2}{\sigma^2} \quad (1),$$

$I'(B_i)_{YYY}$ $YYY=\{EXP, SIM\}$ are experimental and simulated first derivative spectra, $N=1500$ is the number of experimental points representing the whole spectra, σ^2 is the experimental variance estimated from the tail of spectra. Minimization of χ^2 is done with the Matlab function `fminsearch`, (using the Nelder-Mead simplex algorithm). For best fit parameters see Table 1.

Table S1. EPR parameters obtained by simulation of the frozen solution (120 K) spectra of Cu(II)porphyrins **1** and **2**, where σ_R is the homogenous broadening, $\sigma_{H\perp}$ and $\sigma_{H//}$ are orientation dependent broadening terms (so called H-strains). All magnetic parameters are given in Gauss. Note that χ^2 is larger for porphyrin **2**, the main reason for this comes from a smaller σ^2 for experiment **2**, *i.e.* the mean square error (nominator in (1)) is similar for the two experiments.

Porphyrin	χ^2	σ_R	$\sigma_{H\perp}$	$\sigma_{H//}$	g_{\perp}	$g_{//}$	A_{\perp} (⁶³ Cu)	$A_{//}$ (⁶³ Cu)	A_{\perp} (¹⁴ N)	$A_{//}$ (¹⁴ N)
Cu(DPP) 1	148	9.8	0.03	15.1	2.045	2.191	20.6	211.9	17.1	13.8
Cu(TPP) 2	500	11.9	0.04	10.6	2.046	2.189	20.9	210.5	16.8	14.5

Note that there are several routes for which parameter estimation in Table S1 can be done, both at the level of approximation in the numerical line shape calculation as well as in the number and type of phenomenological broadening parameters (here σ_R , $\sigma_{H\perp}$ and $\sigma_{H//}$ are used). However, above procedure was found in a recent study³ to give the set of spin-Hamiltonian parameters for porphyrin

1 that also consistently explains the lineshapes in fluid solution 197-293 K. Note first, the liquid state study was performed with rigorous non-perturbative simulation techniques. Secondly, both porphyrins were prepared by identical procedures, thus providing confidence in both parameter sets in Table S1. The agreement with the liquid state study also indicates that no significant freezing artefact was introduced upon freezing the sample.⁴

We provide qualitative simulation of fluid solution spectra in Figure S2 and S3 and computed with the expression $a + bm_1 + cm_1^2$ for the linewidths (L/W) of the copper peaks.⁵ The lack of quantitative predictive power comes from a slow molecular tumbling on EPR time scale. A detailed study of fluid solution copper porphyrin is performed elsewhere.³

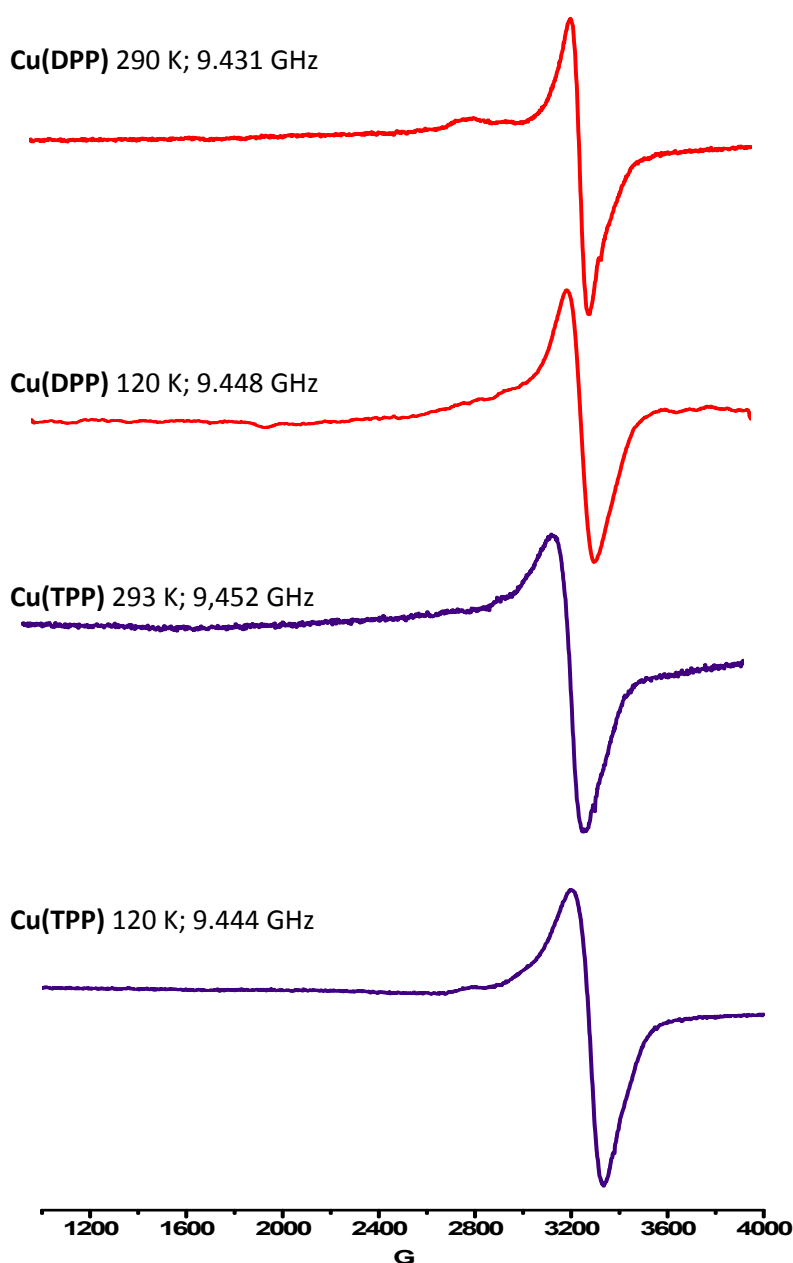


Figure S1: 1st derivative EPR spectra of powder samples of **Cu(DPP)** and **Cu(TPP)** at ambient and frozen temperatures. Spectra were acquired with 3.99 mW microwave power, 2 Gauss modulation amplitude, and approx. 9.4 GHz microwave frequency.

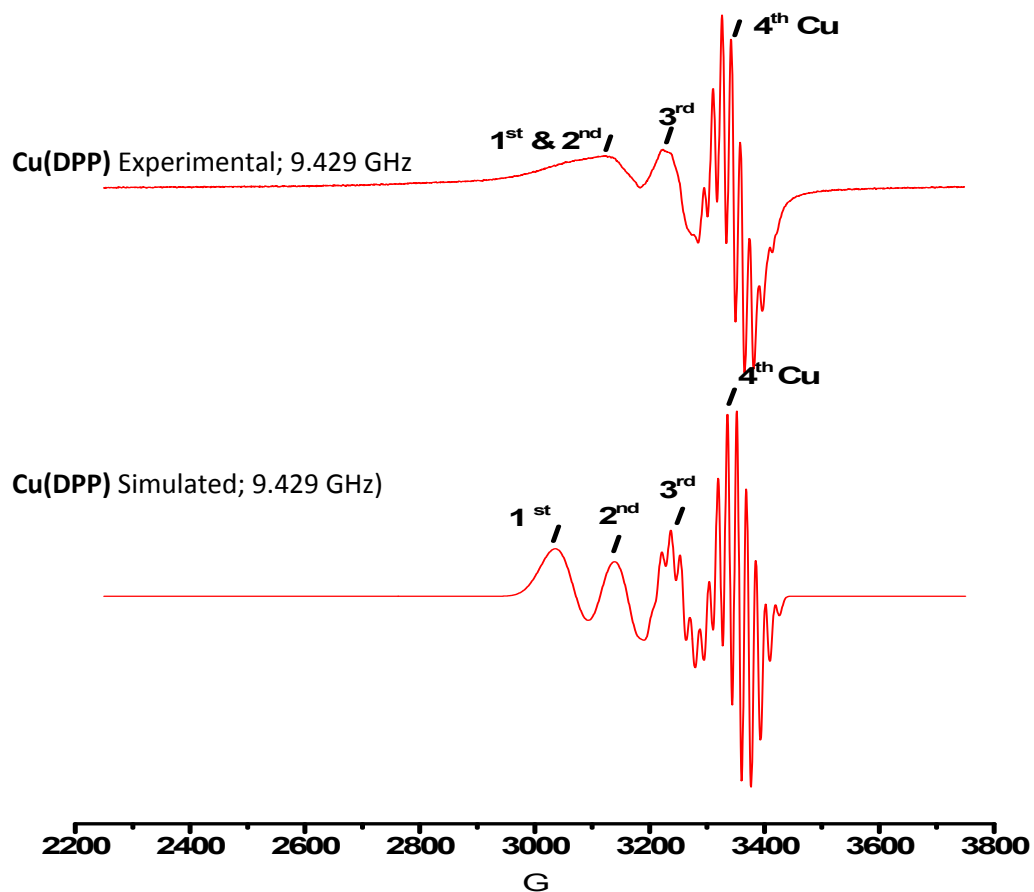


Figure S2: Experimental and simulated 1st derivative solution spectra of **Cu(DPP)**, ⁶³Cu (100 %) in DCM:toluene 9:1 have $g_{\text{iso}} = 2.095$, $A_{\text{iso}}(^{63}\text{Cu}) = 90$ Gauss, $A_{\text{iso}}(^{14}\text{N}) = 16$ Gauss, Lorentzian/Gaussian lineshape = 1, $L/W = a + bm_1 + cm_1^2$, $a = 20$ G, $b = 10$ G, $c = 3$ G.

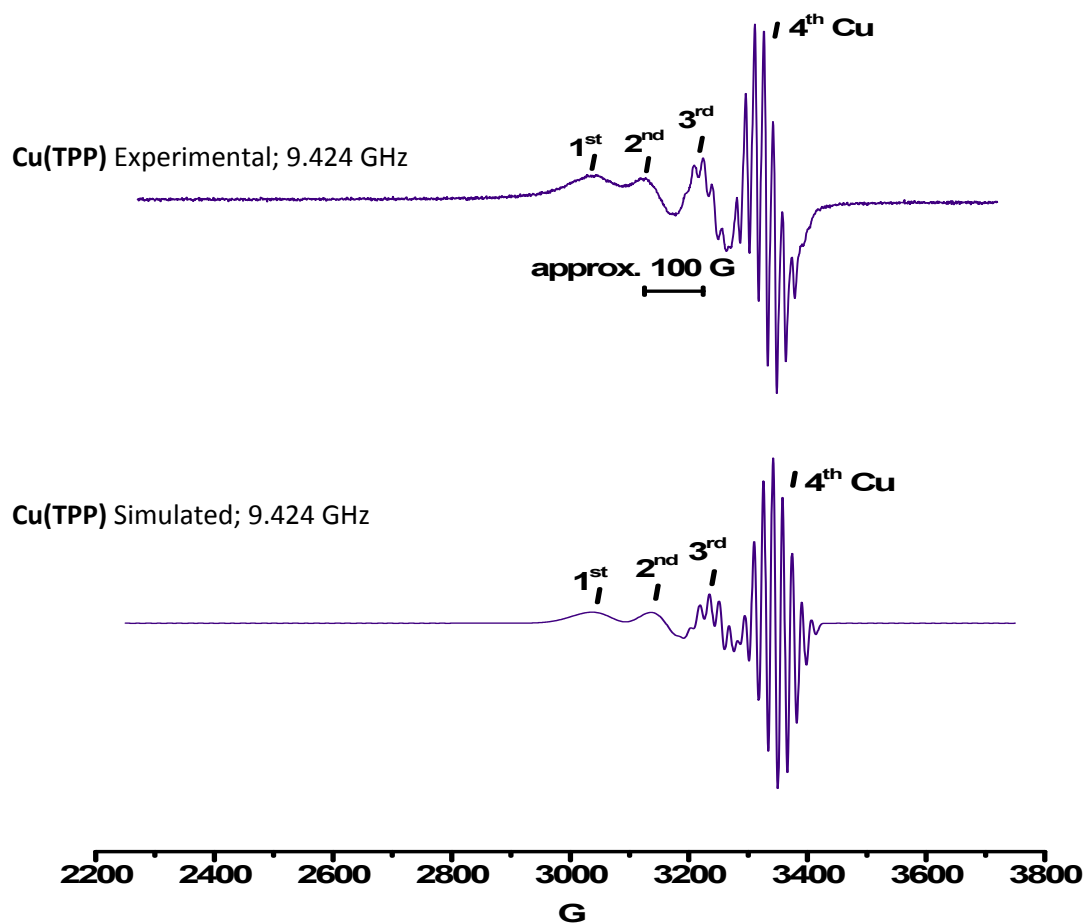


Figure S3: Experimental and simulated 1st derivative solution spectra of **Cu(TPP)**, ⁶³Cu (100 %) in DCM:toluene 9:1 have $g_{\text{iso}}=2.095$, $A_{\text{iso}}(^{63}\text{Cu})=88$ G, $A_{\text{iso}}(^{14}\text{N})=15.8$ G, L/G lineshape=1, L/W= $a + bm_1 + cm_1^2$, $a=23$ G, $b= 21$ G, $c= 8$ G.

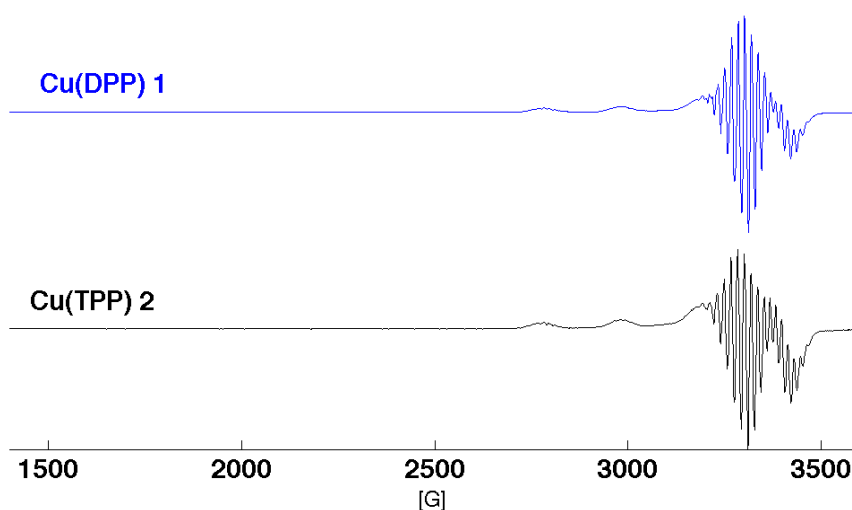


Figure S4: Full spectral width of the EPR spectra of **1** and **2** to show absence of half-field signal in the building blocks in organic solvents.

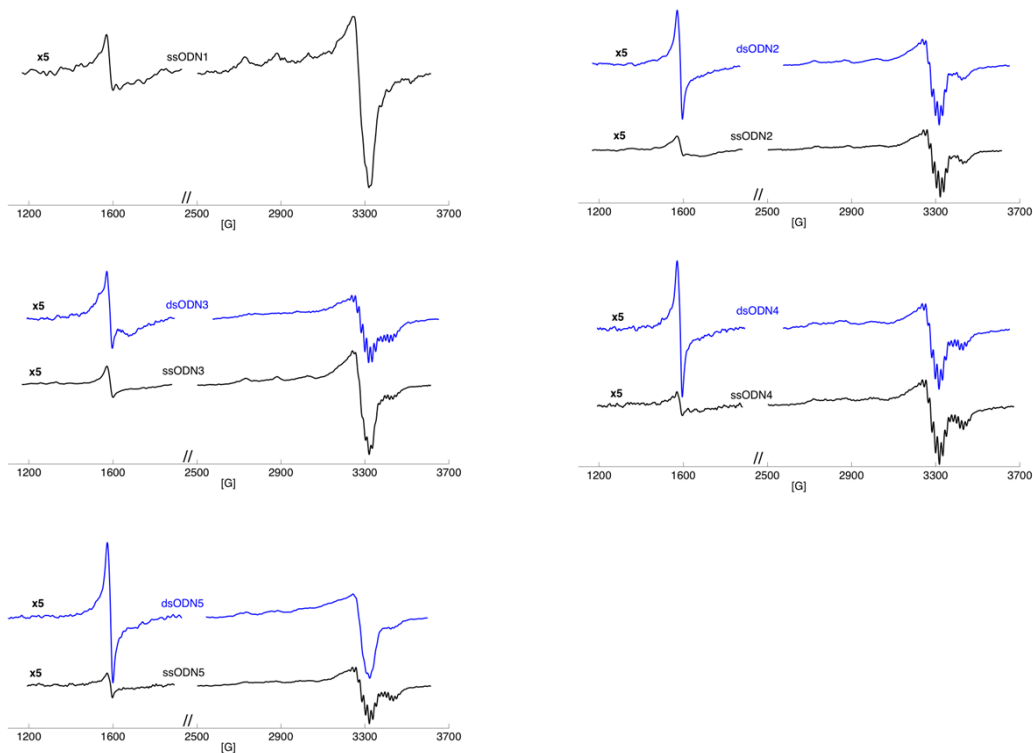


Figure S5: 1st derivative frozen solution EPR spectra of 300 μ M porphyrin-DNA single and double strands in water at 120 K. Spectra were acquired with 3.99 mW microwave power, 5 Gauss modulation amplitude and approx. 9.4 GHz microwave frequency. Spectra are baseline corrected with first order polynomial and scaled with the area of the main transition absorption spectra. The half field transition (\sim 1600 G) is amplified 5 times.

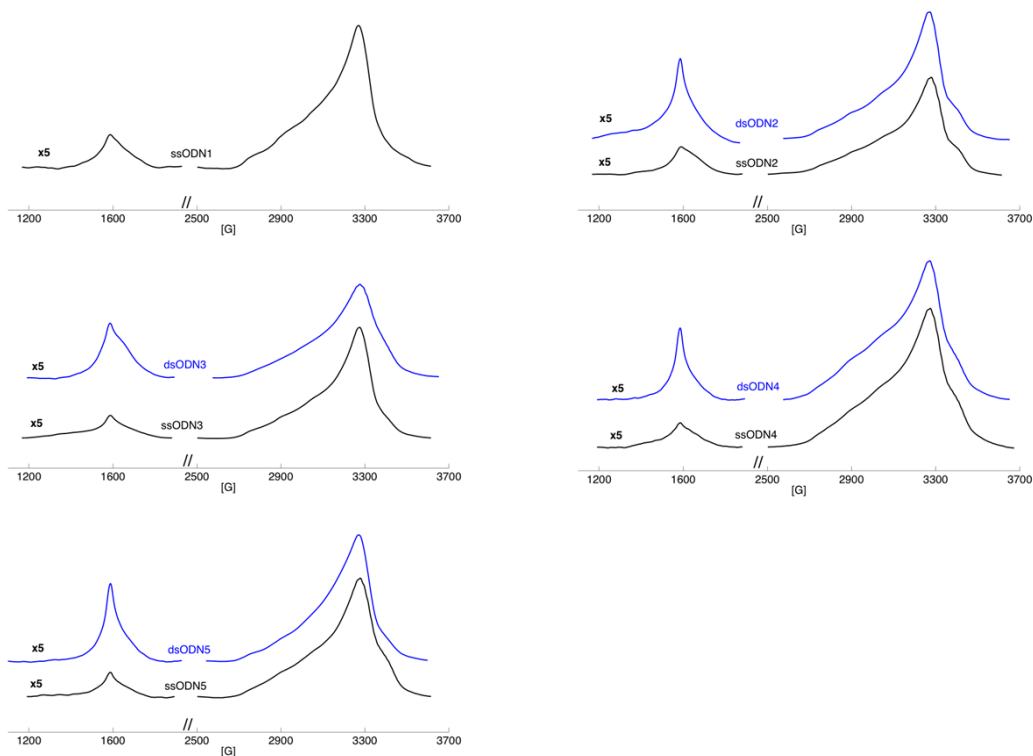


Figure S6: The spectra of Figure S5 integrated, providing absorption spectra. The half field transition is amplified 5 times.

5 Cu-Cu Distance estimation ODN1-ODN5

ssODN spectra is baseline corrected with a first order polynomial ($ax+b$). 1st-derivative spectrum (Figure S5) is integrated to provide the absorption spectra in Figure S6. Finally the absorption spectra (Figure S6) are integrated to provide $\text{area}(|\Delta M_s|=2)$ and $\text{area}(|\Delta M_s|=1)$ with:

$$I_{\text{rel}} = \text{area}(|\Delta M_s|=2)/\text{area}(|\Delta M_s|=1). \quad (2)$$

Under the assumption of a two electron spin interaction the estimated distance between interacting spins is obtained from $I_{\text{rel}}=K/r^6$, where a K value particularly calibrated to copper complexes is used⁶ ($K=256.7 \text{ (\AA}^6)$). Alternatively $K_0=21 \text{ (\AA}^6)$ given by the general form⁷ $K_0=(19.5 + 10.9\Delta g)(9.1/v)^2$, may be used. Analysing I_{rel} with K and K_0 give distances in the range 4-5Å and 2.6-3.4Å respectively for all samples (data not shown). These very short distances (4-5Å) correspond to DD interaction of 190 G (in the range 148-290 G). Simply considering such strong interaction (leaving the interpretation in terms of distances aside), is inconsistent with what we see in main transition, lacking splitting of this magnitude. To proceed we analyse the main transition.

6 Spectral properties from determined distances

The estimated single distances translate into typically 190 G DD interaction. Thus the question arises if this magnitude of interaction is represented in the main transition. Here we make a line shape estimate assuming a single Cu(II)-Cu(II) system with two electrons with spin 1/2 and two ⁶³Cu spin 3/2. The individual g and A tensors are taken from Table S1 and are assumed to be diagonal. The spin-spin interaction tensor (D_{xx}, D_{yy}, D_{zz}) are allowed to be rotated relative the Z-axis of the g-tensor with polar angle θ as a fitting variable. The line shape fitted to the absorption spectra of ssODN3 main transition is given in Figure S8, with spin-spin interaction, polar angle and isotropic line widths as fitted variables. In this approach antisymmetric exchange and N nuclei excluded.

The fitted result translates into isotropic exchange coupling 14 G, rombicity $D_{xx}-D_{yy} = 1.2 \text{ G}$, $DD=51 \text{ G}$, $\theta=10$ degrees and isotropic line width 96 G. The relative intensities for the simulations are $I_{\text{rel}}=0.0002$, a factor of 100 smaller than experimental observation.

Although the line shape study in figure S8, have room for improvement, for instance by exploring additional nitrogen nuclei, the discrepancy in DD predicted by half field intensity and spectral analysis is evidence that single pair of Cu(II)-Cu(II) can not explain the EPR observation. We conclude, omitting the details of the fitted result, the DD interaction cannot be larger than 66 G, in order not to introduce a larger DD splitting in the line shape. We take this largest interaction (shortest distance) forward to reach a physically consistent interpretation with a multi distance model below.

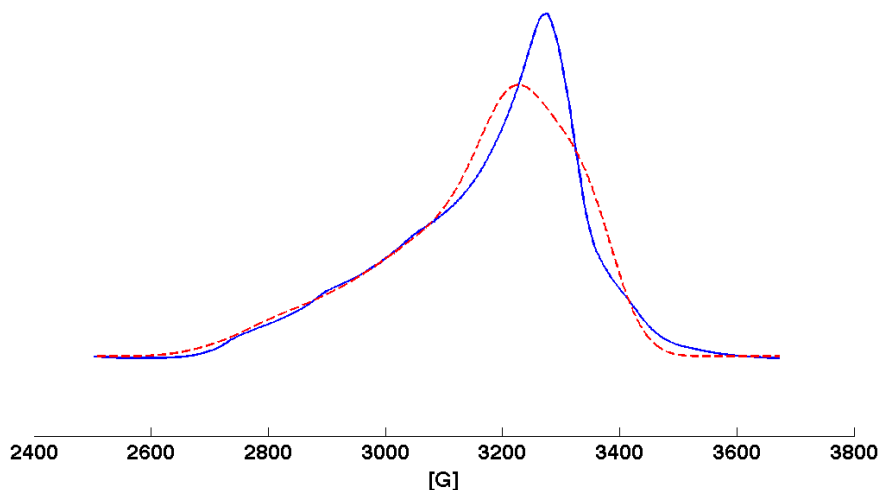


Figure S7: The absorption spectra for ssODN3 and simulated electron spin-spin interaction with black-solid and red-dashed line respectively. The simulated spin system consists of two electron spins and two nuclear 3/2 (Cu(II)) spins. The simulation is performed with the assumptions of equal and diagonal g and A tensors with parameters taken from Table S1. The result of a fitting procedure is isotropic exchange coupling 14 G, rombicity $D_{xx}-D_{yy} = 1.2G$, $DD=51$ G and isotropic line width 96 G.

7 Multiple pair distance model

For a cluster of Cu(II) we may construct a multi distance model. With a weak dipole-dipole interaction compared to the Zeeman interaction, perturbation theory provides the relative half field intensity proportional to c^2 , with

$$c = \mu_B \sum_{i<j}^N r_{ij}^{-3} / B, \quad (3)$$

where B is the magnetic field, N is the total number of electron spin interactions in the cluster, see Ref 7, page 137. To arrive at a tractable model that reflects the number of interactions, we consider an effective distance r_{eff} such that I_{rel} is given by

$$I_{rel} = K_0 \left(\frac{N}{r_{eff}^3} \right)^2, \quad (4)$$

where $K_0=21$ (\AA^6).

In table S2 up to eight ODNs are listed, together with total number of interactions N, note that ds and ssODN3 and ssODN1 have *one* porphyrin per ODN, where as the remaining have *two*.

Table S2 The numbers of interactions (N) for cluster of 2-8 ODNs.

#ODN	1 Cu(II)/ODN		2 Cu(II)/ODN	
	#Cu(II)	N	#Cu(II)	N
2	2	1	4	6
3	3	3	6	15
4	4	6	8	28
5	5	10	10	45
6	6	15	12	66
7	7	21	14	91
8	8	28	16	120

The table S3 summarise the result for 1-8 ODNs. First we note that for 1 pair of of ODN there is not enough interaction for the model to describe I_{rel} . For 3-4 ODNs, the single Cu(II)-porphyrin ODN's ssODN1 and ss and dsODN3 still have too weak DD interaction for model to explain the data. Hence, the distance r_{eff} would need to be shorter. However, the main transition line shape as is shown in figure S7 contradicts this. We note that EPR study cannot on its own rule out larger. However, if the dimensionality predicted in SAXS study⁸ is valid also for these samples, clusters larger than 6-ODNs can be ruled out.

To estimate the error, additional distances are calculated with base line correction (see parameters a,b in sec. 5) chosen to give spectra with a clearly distorted shape (spectra not shown) and comparing theses distances with those provided in Table S3. This suggests that the two significant digits in r_{eff} are valid.

Comparing the ds and ss data we note a longer effective distance for ss-data as is consistent with the expected larger flexibility of single strands causing longer distances.

Table S3. Relative half-field intensity and computed distance for Cu(II)porphyrin-DNA as single strand (ss) and double stranded (ds) systems from experimental frozen solution spectra. r_{eff} is an effective distance fulfilling $r_{\text{eff}} > 6.5 \text{ \AA}$. Total number of interactions depend on number of porphyrins in base sequences, see table S2. Letters S denote failing model where the half field intensity is too small.

Compound	Conc. (μM)	Local base-sequence	I_{rel}	$r_{\text{eff}}(\text{\AA})$ 2-ODN	$r_{\text{eff}}(\text{\AA})$ 3-ODN	$r_{\text{eff}}(\text{\AA})$ 4-ODN	$r_{\text{eff}}(\text{\AA})$ 5-ODN	$r_{\text{eff}}(\text{\AA})$ 6-ODN	$r_{\text{eff}}(\text{\AA})$ 7-ODN	$r_{\text{eff}}(\text{\AA})$ 8-ODN
ssODN1	300	A TPT A	0.024	S	S	S	6.7(2)	7.6(8)	8.5(8)	9.4(4)
	100		0.024		S	S	6.6(8)	7.6(3)	8.5(2)	9.3(9)
ssODN2	300	A PAP A	0.032	S	7.3(0)	8.9(6)	10.(5)	11.(9)	13.(3)	14.(5)
dsODN2	300		0.064	S	S	7.9(8)	9.3(7)	10.(6)	11.(8)	13.(0)
ssODN3	300	A PAT A	0.030	S	S	S	S	7.3(9)	8..2(7)	9.0(9)
dsODN3	300		0.056	S	S	S	S	6.6(5)	7.4(3)	8.1(2)
	100		0.063	S	S	S	S	6.5(0)	7.3(0)	8.0(0)
ssODN4	300	A PAP A	0.017	S	8.0(8)	9.9(4)	11.(6)	13.(2)	14.(7)	16.(1)
dsODN4	300		0.031	S	7.3(3)	8.9(8)	10.(5)	12.(0)	13.(3)	14.(6)
	100		0.04	S	6.9(9)	8.6(3)	10.(1)	11.(5)	12.(8)	14.(0)
ssODN5	300	TP PAT	0.019	S	7.9(7)	9.8(3)	11.(5)	13.(1)	14.(5)	15.(9)
dsODN5	300		0.048	S	6.8(2)	8.3(8)	9.8(1)	11.(1)	12.(4)	13.(6)

References:

1. a) Bouamaied, I.; Nguyen, T.; Rühl, T.; Stulz, E. *Org. Biomol. Chem.* **2008**, *6*, 3888-3891; b) Brewer, A.; Siligardi, G.; Neylon, C.; Stulz, E. *Org. Biomol. Chem.* **2011**, *9*, 777-782.
2. S. Stoll and A. Schweiger, *J. Magn. Reson.*, **2006**, *178*, 42–55.
3. Håkansson, P.; ThaoNguyen N.; Nair P. B. ; Edge R.; Stulz E. *Phys. Chem. Chem. Phys.* **2013**, *15*, 10930-10941.
4. Hyde, J.S.; Froncisz, W. *Ann. Rev. Biophys. Bioeng.* **1982**, *11*, 391.
5. Sealy, R. C.; Hyde, J.S.; Félix, C.C.; Menon, I.A.; Prota, G.; Swartz, H. M.; Persad, S.; Haberman, H. F., *Proc. Natl. Acad. Sci. U. S. A.* **1982**, *79*(9), 2885-2889.
6. Svorec, J.; Valko, M.; Moncol, J.; Mazúr, M.; Melník, M.; Telsler, J., *Transition Met. Chem.* **2007**, *34*, 129-134.
7. A. Bencini and D. Gatteschi, *Electron Paramagnetic Resonance of Exchange Coupled Systems*, Springer-Verlag GmbH, New York, 1990.
8. A. Brewer, G. Siligardi, C. Neylon and E. Stulz, *Org. Biomol. Chem.*, 2011, **9**, 777-782.